Finally, we assume the volume dependence of W is given by Heine's[23] results

$$\frac{\partial \ln W}{\partial \ln V} = -\frac{5}{3} \quad . \tag{5}$$

Using the above results, Eqs. (3)–(5), the volume dependence of $\bar{I}$, Eq. (2), is[12]

$$\frac{\partial \ln \bar{I}}{\partial \ln V} = \frac{5}{3}\,\frac{I}{I_b} \quad , \tag{6}$$

which is independent of β and γ and where here I_b is assumed independent of volume. For the density of states of the form given by Eq. (4), it can be shown that $T_F \sim W$, and hence from Eq. (5), $\partial \ln T_F / \partial \ln V = -\frac{5}{3}$. Using Eqs. (1), (2), (5), and (6) the volume dependence of T_c becomes

$$\frac{\partial \ln T_c}{\partial \ln V} \equiv \Gamma$$

$$= -\tfrac{5}{3} + \tfrac{5}{6}\,(\bar{I}-1)^{-1}(I/I_b) \,. \tag{7}$$

In terms of pressure, Eq. (7) can be written as

$$\frac{\partial T_c}{\partial P} = \tfrac{5}{3}\kappa T_c - \tfrac{5}{6}\kappa\,\frac{I}{\bar{I} I_b}\,\frac{T_F^2}{T_c} \quad , \tag{8}$$

where κ is the volume compressibility and we have used Eq. (1).

We shall now show how pressure measurements of T_c can be used to determine a maximum value for $\bar{I}$ and a minimum value for T_F. The maximum value that I can have is the bare exchange value I_b; thus, the maximum value for the ratio I/I_b is one. Hence, the experimental value of Γ can be used to determine the maximum values of $\bar{I}$. From Eq. (7) we have

$$\bar{I}_{\max} = 1 + \tfrac{5}{6}\,(\Gamma + \tfrac{5}{3})^{-1} \quad . \tag{9}$$

Then using values for $\bar{I}$ obtained from Eq. (9) we can obtain a minimum value for T_F using Eq. (1).

For weak itinerant-electron FM's $\bar{I} \gtrsim 1.0$ and for weak electron-correlation effects $I/I_b \cong 1.0$, the second term in Eq. (7) is dominant, and from Eq. (8) we have $\partial T_c/\partial P \sim -1/T_c$. Examples of weak itinerant-electron FM's are the Fe-Ni, Fe-Pt, and Fe-Pd Invar alloys where it has been experimentally observed that $\partial T_c/\partial P \cong -\text{const}/T_c$.[24] For strong itinerant-electron FM's $\bar{I} > 1$ and for strong correlation effects $I/I_b < 1$ such that the first term in Eq. (7) is dominant, and from Eq. (8) we have $\partial T_c/\partial P \sim T_c$. An example of a strong itinerant-electron FM is Ni, where it is found that $\partial T_c/\partial P = \frac{5}{3}\kappa T_c \cong 0.68\ ^\circ\text{K/kbar}$ in good agreement with experimental values of 0.32–$0.42\ ^\circ\text{K/kbar}$.[9] It is noteworthy that in the limit of weak itinerant-electron FM and for large Γ such that $|\Gamma| \gg \frac{5}{3}$ and neglecting the volume dependence of I_b, the results of this paper reduce to the results given previouly by Wohlfarth and Bartel.[12]

The localized and the itinerant, or collective, descriptions of magnetic electrons have been investigated by Goodenough.[25] He considered the case of one d electron per relevant d orbital which correponds to a half-filled band or to a half-filled localized orbital, and the magnetic order is antiferromagnetic (AFM). In the absence of competing exchange interactions, the Néel temperature T_N for localized-electron AFM increases with the transfer integral b since the exchange interaction is proportional to b^2; whereas, it has been shown that T_N for a band AFM decreases with increasing bandwidth[25,26] where the bandwidth is proportional to b. Goodenough concludes that the magnetic moment and T_N should vary continuously in going from a localized to a band description. We expect b to increase with increasing pressure; hence, we expect that for the localized electron description T_N should increase with increasing pressure, and for the itinerant description T_N should decrease with increasing pressure.[26] Furthermore, we expect that the general arguments for an AFM apply to the FM case of interest here. The observed decrease in the FM-to-PM transition temperature in the $MnAs_xSb_{1-x}$ compounds suggests that the itinerant-electron description is the appropriate one. Although these compounds are anisotropic, the isotropic model discussed in this paper describes the pressure effects quite well.

2. *Analysis of Experimental Results*

In Fig. 6, $\partial T_c/\partial P$ is plotted as a function of T_c for the $MnAs_xSb_{1-x}$ solid solutions in the concentration range $0 \leq x \leq 0.8$. For comparison, the Fe-Ni, Fe-Pd, and Fe-Pt Invar alloy data of Wayne and Bartel[24] are included. Similar to the Invar alloys, we observe a T_c^{-1} type of behavior as predicted by Eq. (8) when the second term in Eq. (8) dominates.

The volume derivative of T_c is calculated from $\partial T_c/\partial P$ where the compressibility for the solid solutions was obtained by a linear extrapolation between the values of $(2.5 \pm 0.5) \times 10^{-3}$ kbar^{-1} for MnSb[27] and 4.55×10^{-3} kbar^{-1} for MnAs.[1] The values for Γ are given in Table I. We observe that the values of Γ increase with increasing As concentration and that the magnitude of Γ is of the same order of magnitude as the first term in Eq. (7). In previous works on the Invar alloys[11,12] and $ZrZn_2$,[9-12] it was observed that $\Gamma \gg \frac{5}{3}$ and so the first term of Eq. (7) could be neglected. In the case of the $MnAs_xSb_{1-x}$ solid solutions, this factor of $\frac{5}{3}$ must be included in any calculation of band parameters.

In Table I, we give the results of the calculation of $\bar{I}_{\max}$ from Eq. (9) for the solid solutions $0 \leq x \leq 0.80$. The quoted error in the compressibility for MnSb will introduce an uncertainty of ± 0.03 in the value for $\bar{I}_{\max}$. We observe that $\bar{I}_{\max}$ decreases with increasing As concentration. According to Wohl-

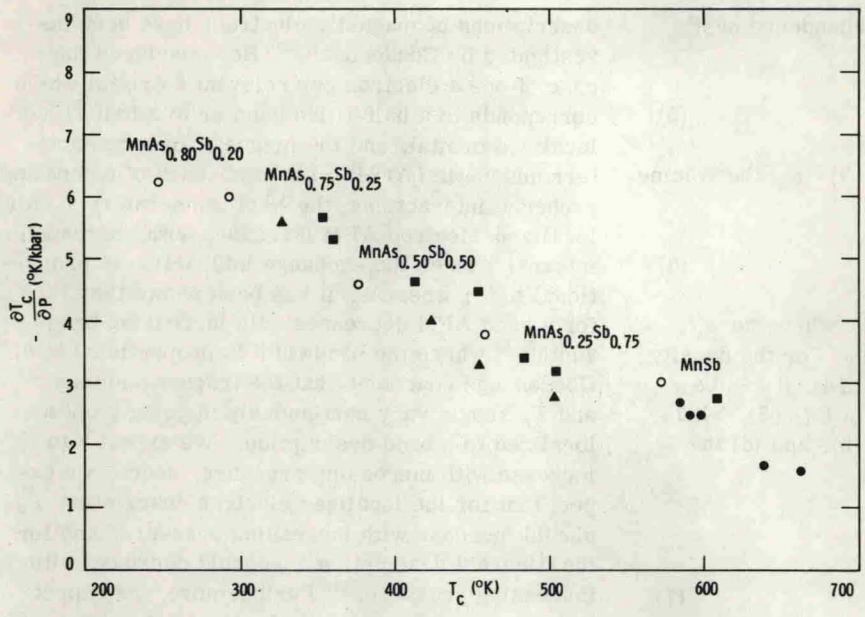

FIG. 6. A comparison of $\partial T_c/\partial P$-vs-T_c plots for various alloy systems. Open circle, $MnAs_xSb_{1-x}$; triangles Fe-Pt; solid circle, Fe-Pd; and square, Fe-Ni.

farth's[28] classification, these values of $\bar{I}_{max}$ indicate that MnSb is approaching a strong itinerant FM, and the solid solutions are becoming weaker itinerant FM's with increasing As concentration. These values of $\bar{I}_{max}$ for the $MnAs_xSb_{1-x}$ solid solutions are comparable with the values for the Invar alloys.[29]

From Eq. (1), and using the value of $\bar{I}$ and T_c for MnSb from Table I, we calculate $T_F = 1380\,^\circ$K. Thus for MnSb we see that $T_c \cong 0.4T_F$ which indicates the Sommerfeld expansion is converging; however, the convergence is slower than one would desire. For the materials with $x > 0$, the convergence is more rapid than for $x = 0$.

Using Eqs. (1)–(4), we can express T_c as a function of the bandwidth W where we assume $T_F \sim W$. Then using the value of $T_c = 572\,^\circ$K and the value of $\bar{I}_{max}$ from Table I for MnSb, we can calculate T_c as a function of W. The results of these calculations are shown in Fig. 7. These results are independent of the value of I/I_b,[30] but do not include effects of any volume dependence of I_b. Note the critical bandwidth such that for $W/W_0 \geq 1.206$ we do not have FM order, and note the quadratic dependence of T_c on W for $W/W_0 \lesssim 1.206$. Using the available x-ray data[31] to estimate W/W_0 and using the experimental values for T_c we show, in Fig. 7, the experimental results of T_c as a function of W/W_0. For $x = 0.25$ we calculate $T_c = 474\,^\circ$K and $\bar{I} = 1.110$ in fair agreement with the experimental values. For the solid solutions $x > 0.25$ the agreement is only qualitative. This disagreement is not too surprising because of the large differences in unit-cell volumes for the various compositions. For these large volume differences one might expect significant changes in the crystal-field splittings, and consequently significant changes in the electronic wave functions. Any volume dependence of I_b would modify the results shown in Fig. 7. Lacking specific-heat, susceptibility, and magnetostriction data for these materials, we cannot determine $N(\epsilon_F)$, I, I_b, and any volume dependence of I_b individually. In addition, as we shall point out below, we expect rather large electron-lattice and exchange-striction interactions for these materials, particularly for the solid solutions $x \gtrsim 0.80$. Electron-lattice and exchange-striction effects have not been included in the calculations displayed in Fig. 7.

Sirota and Vasilev[4] have observed a Curie-Weiss type of behavior in the PM region for MnSb, with a Curie constant, $C_M = 1.3$ emu mole^{-1} Oe^{-1} °K^{-1}. According to the itinerant FM model of Wohlfarth[9] the susceptibility in the temperature region $T_F \gg T > T_c$ and for $T \to T_c$ can be written as $\chi \simeq \chi_0 T_c \times (T - T_c)^{-1}$ which is a Curie-Weiss type of behavior where the Curie constant C_M is given by $C_M = \chi_0 T_c$. The quantity χ_0 is proportional to $N(\epsilon_F)(\bar{I} - 1)^{-1}$.[9] For MnSb, χ_0 can be calculated to give $\chi_0 = 0.227$

TABLE I. Curie temperature T_c, $\Gamma \equiv \partial \ln T_c/\partial \ln V$, and $\bar{I}_{max}$, as calculated from Eq. (9), for various solid solutions of $MnAs_xSb_{1-x}$ in the second-order region.

x(at.% As)	T_c	Γ	$\bar{I}_{max}$
0.00	572	2.38	1.206
0.25	458	2.97	1.180
0.50	375	3.63	1.157
0.75	292	5.18	1.122
0.80	247	6.20	1.106